

UNCLASSIFIED

AD 401 191

*Reproduced
by the*

DEFENSE DOCUMENTATION CENTER

FOR

SCIENTIFIC AND TECHNICAL INFORMATION

CAMERON STATION, ALEXANDRIA, VIRGINIA

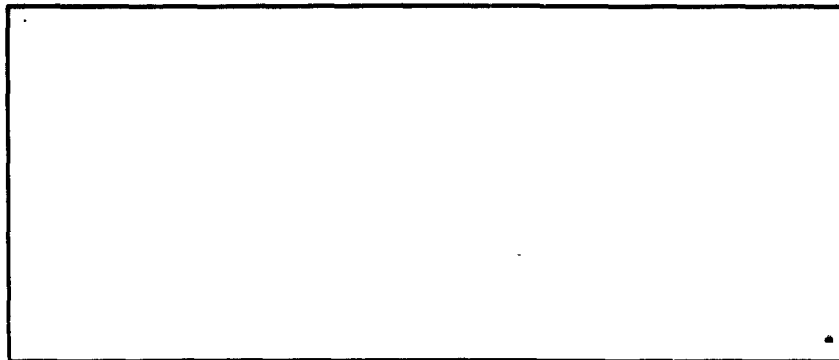


UNCLASSIFIED

NOTICE: When government or other drawings, specifications or other data are used for any purpose other than in connection with a definitely related government procurement operation, the U. S. Government thereby incurs no responsibility, nor any obligation whatsoever; and the fact that the Government may have formulated, furnished, or in any way supplied the said drawings, specifications, or other data is not to be regarded by implication or otherwise as in any manner licensing the holder or any other person or corporation, or conveying any rights or permission to manufacture, use or sell any patented invention that may in any way be related thereto.

401 191

CATALOGED BY ASTIA
AS AD NO 401191



ADVANCED KINETICS

63-3-2

[Faint, illegible handwritten text]

AFCL - 62 - 718

A D V A N C E D K I N E T I C S , I N C .

"PRODUCTION OF MILLIMETER AND SUB-MILLIMETER
ELECTROMAGNETIC WAVES BY THE INTERACTION OF
PLASMA AND ELECTRON BEAMS WITH
HIGH INTENSITY PULSED MAGNETS"

Air Force Contract No. 19 - (604) - 7406

EIGHTH QUARTERLY SCIENTIFIC REPORT
FINAL REPORT

Report Period Covered:

April 15, 1962 - July 15, 1962

Supported
by

Physical Electronics Branch
Electronics Material Sciences Laboratories
Electronics Research Directorate
Air Force Cambridge Research Laboratories
Office of Aerospace Research
United States Air Force
Bedford, Mass.

Submitted by:

R. W. Waniek

Ralph W. Waniek
Director of Research

Requests for additional copies by Agencies of the Department of Defense,
their contractors, and other Government agencies should be directed to the:

ARMED SERVICES TECHNICAL INFORMATION AGENCY
ARLINGTON HALL STATION
ARLINGTON 12, VIRGINIA

Department of Defense contractors must be established for ASTIA services
or have their "need-to-know" certified by the cognizant military agency
of their project or contract. All other persons and organizations should
apply to the:

U. S. DEPARTMENT OF COMMERCE
OFFICE OF TECHNICAL SERVICES
WASHINGTON 25, D. C.

A D V A N C E D K I N E T I C S , I N C .

I) INTRODUCTION

The attempt to produce coherent millimeter and sub-millimeter electromagnetic radiation at high power levels by the deceleration of charged particles injected into strong magnetic fields is beset by a number of difficulties related to the source-detection problem in this region of the spectrum. The theoretical study reported on here was initiated to provide foundation and guidance for the concurrent experimental work.

Considering the complexity of the theoretical problem, substantial progress has been made during the contract period. Approximate solutions have been obtained to some of the problems posed, while other problems have been delineated more sharply. Several directions for further work have been uncovered which hold promise of being fruitful. The report presented here summarizes the progress made during the contract period.

II) STATEMENT OF THEORETICAL PROBLEM

The general theoretical problem may be stated as follows: to study the dependence of gyromagnetic radiation production in representative physical systems on the system parameters in order to define the ranges of those parameters which will give optimum performance. (Optimum performance being usually understood to mean maximum power radiated within a certain bandwidth .) During the course of this contract one particular type of experimental system has been used, hence, the theoretical model constructed to represent the physical system

A D V A N C E D K I N E T I C S , I N C .

has been fixed within corresponding limits. Two aspects of the construction of the theoretical model are dealt with in the following two sections: the choice of a representative physical system, and the simplification of the mathematics to obtain tractable equations which still yield meaningful solutions.

A) REPRESENTATIVE PHYSICAL SYSTEM

Basically, the theory must describe the interaction between an ensemble of charged particles and a strong magnetic field.

The character of the ensemble may be simplified by noting that electromagnetic theory dictates that the production of gyromagnetic radiation is primarily a single particle phenomenon, although the characteristics of the emitted radiation are governed by the type of magnetic field as well as by the mode of the particle dynamics in the field. Furthermore, if the ratio of the mean free path of the particles in the ensemble to the local gyromagnetic radius is large, space charge effects may be ignored. Thus, to a first approximation, the ensemble may be taken to consist of non-interacting particles and the theoretical model then involves the interaction of single particles with a strong magnetic field. Note that in such a model, coherence of the emitted radiation depends largely on the initial relative phases of the particles for a given magnetic field.

The magnetic field used in the experimental arrangement was produced

A D V A N C E D K I N E T I C S , I N C .

by a pulsed magnet whose period was long compared to the time spent by the particles in the high field region, hence the field could be taken to be magnetostatic. The field possessed symmetries characteristic of fields produced by many pulsed magnets. Such magnets are symmetric with respect to rotation about an axis passed through the center of the air gap. Moreover, they concentrate their fields within certain regions along the axis of symmetry, frequently displaying a symmetry about an "equatorial" plane passed perpendicular to the axis at the middle of the air gap. It is, in fact, the spatial inhomogeneity of the field thus produced that creates an injection problem because the particles must be introduced into the field at a point remote from the high field region in order to avoid interference of the magnet with the particle source. In such fields, the field magnitude is zero at $\pm \infty$ along the axis and gradually rises to a local maximum at the magnet center.

Thus the representative physical system may be taken to be a group of single particles moving in an axially symmetric, magnetostatic field possessing a local axial maximum at the equatorial plane, and whose magnitude is symmetric with respect to reflections in the equatorial plane.

B) MATHEMATICAL MODEL

The simplifications necessary to establish a tractable mathematical model are considerably more restrictive in nature than those introduced above. The dynamic assumptions introduced are three: (1) only non-relativistic motion will be considered: (2) both the relativistic

A D V A N C E D K I N E T I C S , I N C .

and non-relativistic radiation reaction forces will be neglected, and (3) the actual trajectories will only be dealt with in the paraxial approximation. A discussion of these assumptions may be found in the paper entitled: "The Injection of High Velocity Charged Particles into Strong Magnetic Fields," scheduled for publication in the May, 1963 issue of the Journal of Applied Physics. Certain of the qualitative results do not require assumption (3).

The field behavior of the magnet type outlined above may be adequately represented for the present purposes by a magnetic field whose axial dependence is given by the bell-shaped curve

$$B(0, 0, z) = B_0 / 1 + (z/a)^2 \quad (1)$$

where the z-axis is the axis of symmetry and a denotes the half-width of the curve at half-maximum. This field has the advantage that many of its properties are amenable to analytic treatment.

The production of gyromagnetic radiation is, of course, a relativistic effect in essence, hence due caution must be exercised in the interpretation of results and their application to the study of this phenomenon. Nevertheless, it is felt that the insight gained into the theoretical problem with a non-relativistic treatment can provide valuable guidance for the prosecution of further studies.

Only a few of the basic properties of non-relativistic motion in an axially symmetric magnetostatic field have been worked out in general

A D V A N C E D K I N E T I C S , I N C .

form up to the present time, and recourse must be had in most cases to qualitative considerations, approximate solutions and computer integration of the equations of motion. The research reported here is of the first two types.

C) RESULTS

The results obtained may be classified according to whether they deal with particles which are reflected by the magnetic field, or which penetrate the field to the downstream side of the magnet. Before dealing with these results, two paragraphs are presented containing a brief review of the notation and the basic theory utilized, and an outline of the injection problem.

(A) Review. Calculations are carried out in the standard circular cylindrical coordinate system $(\rho, \theta, \zeta) = (\frac{r}{a}, \theta, \frac{z}{a})$, where a is the field extent parameter defined above. The Lagrangian for an axially symmetric magnetostatic system may be written as:

$$\Lambda = \frac{1}{2} (\dot{\rho}^2 + \rho^2 \dot{\theta}^2 + \dot{\zeta}^2) + \rho \dot{\theta} \alpha(\rho, \zeta) \quad (2)$$

where $\alpha(\rho, \zeta)$ is the dimensionless magnetic vector potential and time measured in units of $(m/e B_0)$. The system is conservative, hence possesses the energy integral

$$\dot{\rho}^2 + \rho^2 \dot{\theta}^2 + \dot{\zeta}^2 = v^2 \quad (3)$$

A D V A N C E D K I N E T I C S , I N C .

(v is the dimensionless velocity), and is axially symmetric hence possesses the angular momentum integral

$$\rho^2 \dot{\theta} + \rho \alpha(\rho, \zeta) = \gamma \quad (4)$$

The latter two equations imply the existence of forbidden zones whose boundaries are defined by the equation

$$\gamma/\rho - \alpha(\rho, \zeta) = \pm v \quad (5)$$

and beyond which the particles of given (v, γ) cannot penetrate.

By restricting consideration to paraxial motion the preceding equation may be solved for ρ to give:

$$\rho_{+++} = v/\Gamma_0 \left[-1 + \sqrt{1 + 2\gamma\Gamma_0/v^2} \right] \quad (6)$$

$$\rho_{-++} = v/\Gamma_0 \left[1 + \sqrt{1 + 2\bar{\gamma}\Gamma_0/v^2} \right] \quad (7)$$

$$\rho_{--+} = v/\Gamma_0 \left[1 + \sqrt{1 - 2\gamma\Gamma_0/v^2} \right] \quad (8)$$

$$\rho_{---} = v/\Gamma_0 \left[1 - \sqrt{1 - 2\bar{\gamma}\Gamma_0/v^2} \right] \quad (9)$$

where Γ_0 is the axial variation of the magnetic field magnitude.

For the bell-shaped field

$$\Gamma_0 = 1/1 + \zeta^2 \quad (10)$$

(b) Injection Problem. During the course of the contract it became apparent that the main theoretical problem would be to predict those values of the appropriate injection parameters which would maximize the radiation emitted in a given spectral region. This involves defining the proper values and ranges of values (allowable spreads) of the coordinates, velocities, principal magnetic field value (B_0) and inter-particle phases,

A D V A N C E D K I N E T I C , I N C .

with the emphasis being placed on determining the values of the coordinates and velocities as the most important parameters. The principal results of this phase of the investigation are to be found in the afore-mentioned paper and will be quoted briefly below.

(c) Reflected Particles. For those particles which do not penetrate to the equatorial plane but are reflected at some point (ρ_r, ζ_r) , some interesting relations may be derived. The following expression for the principal gyromagnetic wavelength, λ_p , may be derived for paraxial motion in a relatively strong magnetic field assuming that most of the radiation is produced near a reflection point where the trajectory may be approximated well by a circular helix:

$$\lambda_p = \left[0.0147 B_o \Gamma_o (\zeta_r) \right]^{-1} \left[\frac{V}{511} + 1 \right] \quad (11)$$

where V is the particle accelerating voltage, and (λ_p, B_o, V) are measured in (mm, Kilogauss, kV), respectively. Since λ_p is usually fixed at the outset, it is more instructive to modify this equation to obtain:

$$V = 511 \left[0.0147 B_o \Gamma_o (\zeta_r) \lambda_p - 1 \right] \quad (12)$$

In this manner, the concept of the threshold field, B_{ot} , comes into existence, defined to be the principal magnetic field which will just allow radiation of wavelength λ_p to be produced at the reflection point. This relation gives the first formal hint that the magnetic field magnitude is the main limiting system parameter with respect to high radiation output.

A D V A N C E D K I N E T I C S , I N C .

The power radiated at the reflection point may be shown to be

$$P = B_o^2 \Gamma_o^2(\zeta_r) \left[(0.0147)^2 B_o^2 \Gamma_o^2(\zeta_r) \lambda_p^2 - 1 \right] \quad (13)$$

where P is measured in ev/ms for each particle. It is this relation which brings out most strongly the importance of making the magnetic field as high as possible; the gain in power at the reflection point for a given wavelength as large as B_o goes much beyond B_{of} . It is important to point out also that the voltage which must match B_o through the second previous equation above must only increase in a linear fashion to keep pace with B_o , hence the magnetic field is again shown to be the most critical system parameter. There exists an unknown factor in this analysis, however. It is not yet known whether the voltage specified by the equation above will be sufficient to allow the particle to penetrate to the particular reflection point, assuming optimum values for the other injection parameters. In order to evaluate this factor the reflection point parameters must be related to the injection point parameters through the solution of the equations of motion. The solution must, however, be a higher order approximation to the trajectories than the paraxial approximation, because no reflection is obtained in paraxial (first-order) approximation. A reformulation of the equations of motion has been carried out to assist this effort. We introduce the generalized coordinates (ψ, χ) in the meridional plane, where ψ is the magnetic scalar potential and χ is the magnetic line of force function. If the time scale is implicitly transformed through the definition

$$d\sigma/d\tau = \Gamma(\rho, \zeta) \quad (14)$$

A D V A N C E D K I N E T I C S , I N C .

then the equations of motion take the form:

$$\dot{\psi} - \frac{\dot{\psi}\dot{\Gamma}}{\Gamma} + \frac{1}{\Gamma} \left(u^2 - \frac{\chi^2}{\rho^2} \right) \frac{\partial \Gamma}{\partial \psi} + \frac{1}{\rho} \frac{\partial \rho}{\partial \psi} \left(u^2 - \dot{\psi}^2 - 2 \frac{\chi^2}{\rho^2} \right) = 0 \quad (15)$$

$$\ddot{\chi} - \frac{\dot{\chi}\dot{\Gamma}}{\Gamma} + \frac{1}{\Gamma} \left(u^2 \rho^2 - \chi^2 \right) \frac{\partial \Gamma}{\partial \chi} + \frac{1}{\rho} \frac{\partial \rho}{\partial \chi} \left(\dot{\chi}^2 - 2\dot{\chi} - \chi^2 \right) + \chi = 0 \quad (16)$$

where the dot now denotes differentiation with respect to σ . Although a simple first order solution to this system has been obtained, no solution has yet been worked out which allows the reflection point to be related to the injection parameters. This constitutes one of the promising directions for further research.

(d) Penetrating Particles. Those particles which attain the equatorial plane with non-zero forward velocity cannot be reflected, hence penetrate the entire field. Their zeroth order archetype trajectory is the paraxial trajectory, which for the bell-shaped field has the form:

$$\rho = c \sqrt{1 + \zeta^2} \sin \left[\sqrt{1 + 1/4 u^2} \cot^{-1} \zeta_0 + \varphi \right] \quad (17)$$

where (c, φ) are constants to be evaluated in terms of the injection parameters. Based upon analysis of the properties of the forbidden zones and paraxial trajectories carried out in the afore-mentioned paper, it is possible to make certain suggestions concerning desirable values of the injection parameters.

A D V A N C E D K I N E T I C S , I N C .

D) CONCLUSIONS

In order for the particles to penetrate to the high field regions where the magnetic field may exert a sizeable effect it seems desirable to inject with: (a) negative angular momentum constant ($\gamma = -\bar{\gamma}$) ; (b) zero angular velocity ($\dot{\theta}_0 = 0$) ; (c) the velocity vector initially pointed along a line of force ($\rho_0^2 = 2\gamma(1 + \zeta_0^2)$), and (d) relatively small values of v ($v = \frac{mv}{eaB_0}$).

Although the basic elements of the injection problem have been derived in a form appropriate to guide an experimental program, a great deal of work remains to be done. More exact trajectories will have to be obtained, which eventually will have to include the radiation reaction effects. Coherence conditions, which have been largely ignored during the present contract, will have to be investigated. These problems and a number of others of varying magnitudes can now be attacked more easily and intelligently as a result of the work reported on above.

III) EXPERIMENTAL STUDIES

The experimental program carried out under the scope of this project was divided into two distinct phases:

- a) the injection studies of high-speed electrons through strong magnetic fields;
- b) the studies on production and detection of cyclotron electromagnetic radiation.

A D V A N C E D K I N E T I C S , I N C .

A) EXPERIMENTAL SET-UP:

The experimental equipment constructed consisted of a pulsed electron source, a pulsed high-field magnet, the vacuum system, the synchronizing electronics and the detection apparatus.

i) the electron sources used were of two types; the cold cathode type was used extensively with a discharge sustained in argon by application of voltages up to 1 KV and currents in excess of 500 mA. Beams of several mA were extracted up to 10 KV under DC conditions. Alternatively, the source could be pulsed by triggering a high-power line discharge circuit, in which case beams of up to 30 KV and about 10 mA were obtained for times of the order of $2\mu\text{s}$. The beams obtained have a diameter of about .2 mm, on impact onto a quartz plate located in the Faraday cup, after traveling through the magnet structure. Hot-filament cathodes were used alternatively to obtain beams of equivalent diameters and currents;

ii) the pulsed high field magnet was a multi-turn structure similar to the ones constructed in the past (see H. Furth and R. W. Waniek, Rev. Sci. Instr. 27, 195, (1956). Fields up to 250 kOe could be obtained over 1" diameter with a field extent parameter of 0.5". After the injection phase was completed, this structure was modified to a Helmholtz geometry of equivalent field strength in order to facilitate the insertion of hardware close to the high field region.

A D V A N C E D K I N E T I C S , I N C .

iii) the vacuum system was constructed so as to allow under usual injection conditions a vacuum of around 10^{-5} Torr. This pressure could be increased to permit a visible observation of beams injected under D.C. conditions. The vacuum in the cold-cathode electron source was around 100 microns and was regulated by a feed valve. All probes were fed through vacuum-tight seals.

iv) the synchronizing electronics allowed a precise timing of the injection pulse with respect to the high field magnet operation. Under transient conditions the electrons were injected close to the maximum of the field pulse to avoid extraneous \dot{B} or $L\dot{I}$ effects in the system. This was about 70 μ s after zero time, the magnet pulse lasting close to 140 μ s. A master signal was used to trigger the magnet circuitry, and after the selected time-delay, the high voltage line was discharged across the accelerating electrode.

v) Two detection systems were adopted, one for each phase of the experiment:

a) during the injection phase a specially shielded Faraday cup was developed with triaxial vacuum-tight connection. The beam current was monitored on a CRO by displaying the voltage pick-up across a 4.7 K Ω resistor joining the cup to ground. The cup could be moved axially about 8", allowing to explore a region extending from 5" below the magnet to the top of the magnet. All CRO readings were made inside a special screened cage.

A D V A N C E D K I N E T I C S , I N C .

b) the radiation detection phase included first an attempt to monitor possible signals with 220 kMc horn and crystal unit. There was considerable doubt that this unit could detect the radiation because of unknown sensitivity of the crystal in the region beyond 300 kMc (= 1 mm), and because of the unknown response time. Experiments were conducted to test, and possibly to improve, sensitivity and response times. IN23 and MA -408 -B crystals were subjected to pulsed signals from an X-band magnetron system (2J51) operating around 19 kMc. Different conditions of reverse bias were attempted. It was noticed that crystals with good sensitivity had good rise-time, and vice-versa. Crystals with good rise-time and sensitivity, however, were generally unaffected by the biasing procedure, whereas poor crystals improved such properties upon biasing. These results together with the consideration of the fragility of the crystals used at G-band indicated that biasing was not advisable in this operation. Rise-times of less than 50 nanoseconds have been measured with a Fischer source directed at the horn.

Since the power expected from the radiator decreases at longer wavelength ($S = v^2 B^2$ and $w = eB/mv$) a critical problem in this experiment was the development of a detection system operating with good efficiency in the region below 500 microns for pulsed signals.

During the last quarter a high sensitivity PEM detector was developed to be operated in liquid helium at fields around 10 kOe. Such system was tested in helium with superconducting fields up to 24 kOe but has not yet

A D V A N C E D K I N E T I C S , I N C .

been connected to the radiator itself. This system is expected to be sensitive in the region of interest.

B) RESULTS

a) INJECTION EXPERIMENTS:

The transmission of electrons through the strong magnetic fields was studied as a function of injection energy and angle. The strength of the magnetic field was varied stepwise to fields beyond 100,000 oersteds. The injection was performed on-axis and off-axis. Also various positions of the detecting Faraday cup and of the injecting electron source were used. The data had to be corrected to eliminate the effect of stray electrons (specular reflection) by evaluating the Larmor radii of electron orbits belonging to each particular injection angle. When such Larmor radii were smaller than the wall dimension, the particular orbit was accepted as falling within the limits of confidence. Orbits touching the walls before passage through the magnet were rejected.

The effect of the forbidden zones on the transmission of the electron beams through the strong field was noticeable. For instance, for 20 KeV injection, the intensity between 0° and 3.5° injection would vary by more than a factor of 2.5 (Fig. 1). Similar conditions are obtained also for the off-axis injection (Fig. 2). The strong magnetic fields increase considerably the transmission. At fields around 20 kOe the current intensity drops by more than a factor of three, at a constant angle, with respect to the zero angle

A D V A N C E D K I N E T I C S , I N C .

injection, and fields in excess of 100 kOe bring back the intensity to the original 0° injection value. All the above injection experiments were carried out with nearly zero (to within the setting accuracy of the electron source) angular momentum.

The results show definitely, therefore, that the forbidden zones impair electron injection (roughly a factor of 5 at 0° and 100 kOe) but that transmission channels existed for the geometry studied at around 3.5°. At such injection angle and under the application of fields around 100,000 Oe, currents of up to 30 μ A could be transmitted corresponding thus to a 2 μ s burst of $3.6 \cdot 10^8$ electrons. For a 10 KeV electron bunch at 100 kOe the cyclotron radiation at roughly 300 kMc would be about $8 \cdot 10^{-14}$ watts/electron yielding a power of about 6 μ W into the solid angle used.

B) DETECTION STUDIES

With an estimated crystal sensitivity of about 1 mV/ μ W at 300 kMc, the experiment with the present electron currents is just marginal and the outcome would clearly depend on problems of amplification. The 220 kMc horn and detector were positioned in a meridional plane outside the magnet and aligned with the center of the same. Special precautions had to be taken to avoid the strong level of noise pick-up during the pulse phase. The signal from the detector was fed via a 175 Ohm cable to a system of 2 cascaded Tektronix preamplifiers, type L. The maximum sensitivity of such a system operated with appropriate termination for optimum noise reduction was 1 mV/cm.

A D V A N C E D K I N E T I C S , I N C .

Under these conditions results were obtained during one run indicating the following signals for injection at 5°:

| <u>Magnetic Field</u> | <u>Peak Signal</u> | <u>Cyclotron Frequency</u> |
|-----------------------|--------------------|---|
| 0 KOe | 20 mV | (background due to induced effects of injected electron pul. |
| 87 KOe | 28 mV | 250 kMc |
| 108 KOe | 42 mV | 310 kMc |

Within the experimental error (estimated at about 10%), the signal would seem to indicate a square power-field relationship, as expected for cyclotron radiation production. The signal obtained at 108 kOe would seem to be clearly above the noise level by a factor of two (at 85 kOe, the expected power is $4 \cdot 10^{-14}$ w/electron versus about 10^{-13} w/electron at 108 kOe). Under the above assumption of a crystal sensitivity of 1 mV/ μ W, such signal would correspond to some 20 μ W of radiated power which is about a factor of 3 higher than the theoretical figure. Such factor, however, might well be attributed to the crystal sensitivity.

CONCLUSION

The evidence seems to indicate that 20 μ W of power have been extracted at 300 kMc from a bunch of 10 keV electrons by cyclotron radiation in a field of 108,000 Oersteds. The presently unknown sensitivity of the detector used could reduce the power figure to the theoretically expected of 6 μ W. The

A D V A N C E D K I N E T I C S , I N C .

encouraging evidence of the above experiments indicates that transmission and radiation can be achieved in high field geometries. The extension of this work must clearly involve higher injection velocities, higher fields and the necessary radiation detector for the shorter wavelengths. The injection at 20 keV through 200,000 Oe is expected to increase the power by a factor of 16 to some 200 μ W radiated at 550 microns or 545 kMc.

FIGURE 1 :

**ELECTRON BEAM CURRENT
v s
ANGLE OF BEAM FROM AXIS**

MAGNETIC FIELD

○ --- 20,000 Oe

△ --- 36,000 Oe

□ --- 41,000 Oe

Ionizing Voltage 1 KV DC

Accelerating Voltage 20 KV (Pulsed)

Injection Point on Axis

5.125" From Field

Faraday Cup 5" From Field

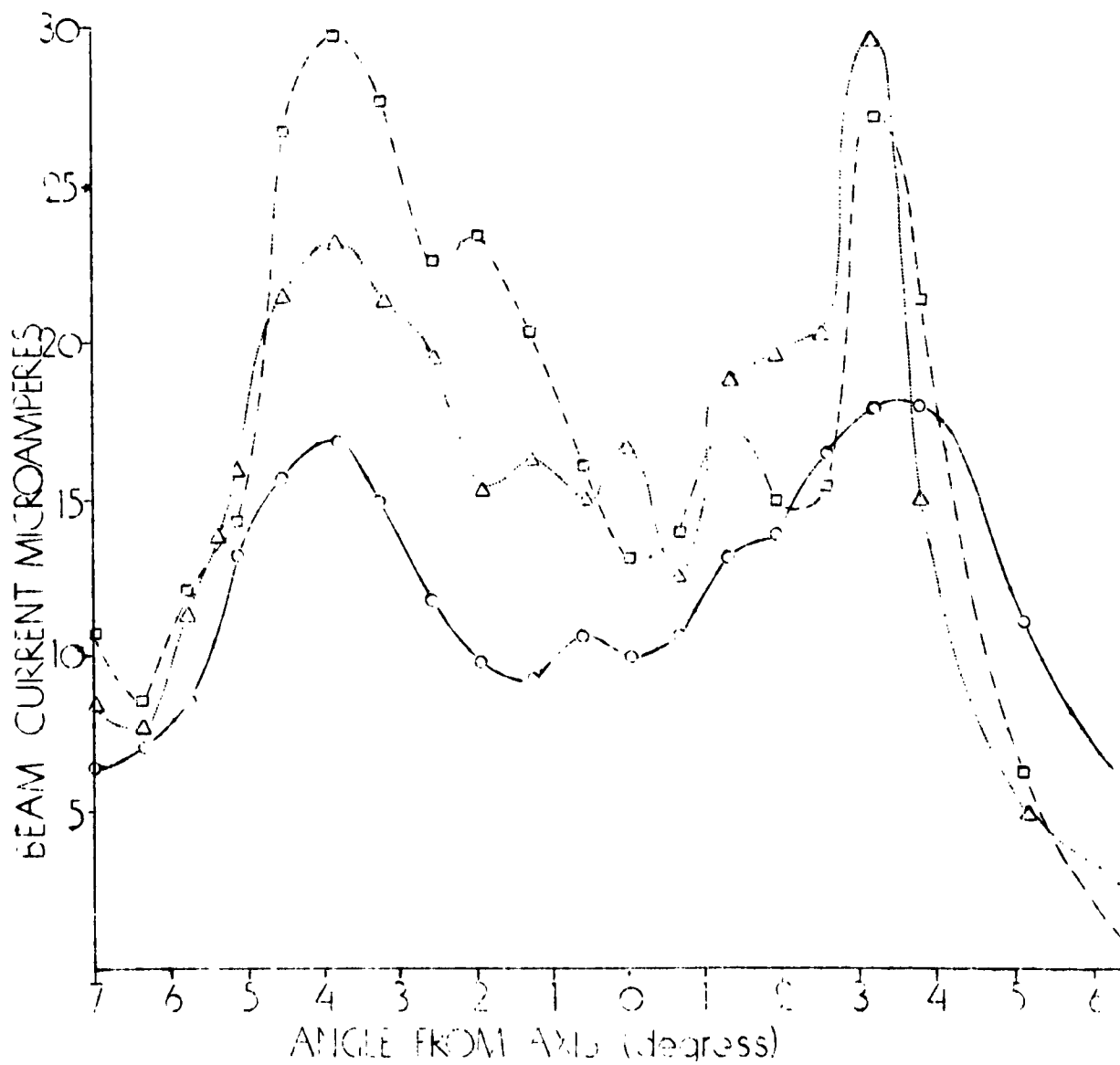
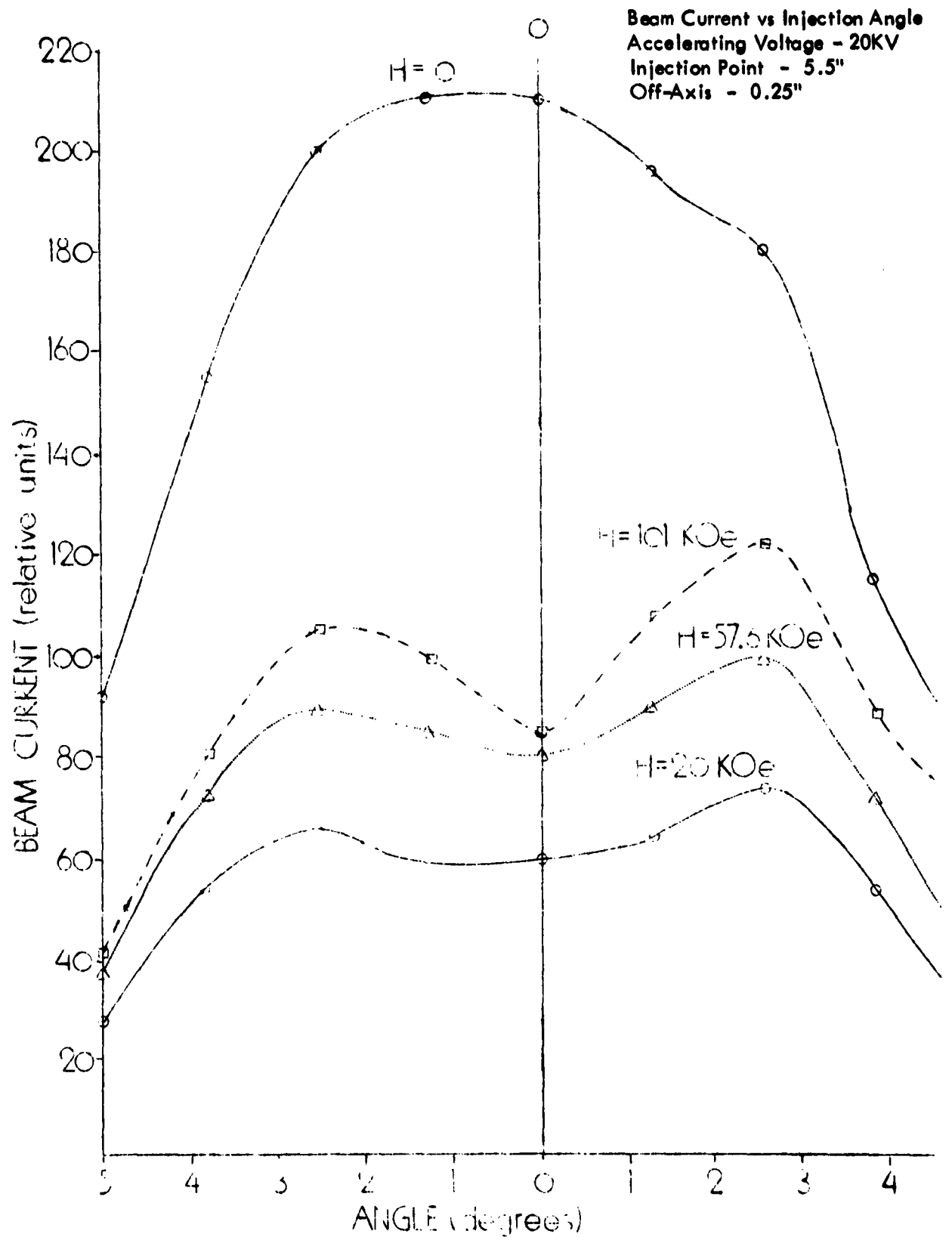


FIGURE 2:



**"THE INJECTION OF HIGH VELOCITY CHARGED PARTICLES
INTO STRONG MAGNETIC FIELDS"***

by

**Malcolm A. MacLeod and Ralph W. Waniek
Advanced Kinetics, Inc.
Costa Mesa, California**

ABSTRACT

Strong magnetic fields are useful in work with high velocity charged particles by virtue of their ability to rotate the particle momentum vector. The degree of usefulness is measured by the extent to which the desired rotations can be produced at the proper positions in the field. It is frequently necessary to inject charged particles into magnetic fields at points remote from these proper positions, in which case the injection parameters which will enable the particles to reach these positions must be specified. For the production of gyromagnetic radiation in axially symmetric magnetostatic fields the proper positions correspond to the high field regions near the symmetry axis. The present introductory study is concerned with delineating approximate injection parameter ranges which will allow the particles to attain the regions of high magnetic field strength in a field whose axial variation is bell-shaped. The single-particle model is adopted, and the results of both qualitative and quantitative investigations are presented.

*Research supported by the Electronics Research Directorate of the Air Force Cambridge Research Laboratories.

A D V A N C E D K I N E T I C S , I N C .

A general formulation of the axially symmetric magnetostatic field forbidden zone theory is given and the useful concept of the paraxial forbidden zones is introduced. This theory is then applied to obtain qualitative answers to the injection problem for the bell-shaped field for both zero and non-zero values of the angular momentum constant. Quantitative relations for the zero angular momentum constant case are obtained using the bell-shaped field paraxial trajectories. A discussion of the limitations of the approximations employed is included.

A D V A N C E D K I N E T I C S , I N C .

1.) INTRODUCTION

The recent development of strong pulsed magnetic fields in the megagauss region^{1,2} has made possible a number of interesting applications, such as coherent electromagnetic radiation production and momentum selection of high energy charged particles³. Many of these applications involve the introduction of a beam or bunch of particles into a pre-existing magnetic field. One of the central problems in such work is the choice of beam injection parameters which will optimize the desired behavior of the particles in the field. This paper is concerned with the zeroth order delineation of those ranges of injection parameters for a particular type of field configuration which will allow the particles to attain regions of high magnetic field strength.

The problem in the forefront during the course of this work has been the production of gyromagnetic radiation, i.e., the production of electromagnetic radiation by the radial acceleration of charged particles in a magnetic field. This is essentially a relativistic effect whereas the mathematical model of the physical situation presented here is of the nonrelativistic variety, hence, due caution must be exercised in the interpretation of results and their application to the study of gyromagnetic radiation production.

In the interest of broad applicability of the results, the current paper deals only with the choice of the particle injection parameters necessary to attain high field regions in a given magnetic field configuration. The choice of the field parameters is determined by the particular application and therefore falls outside the scope of the present discussion.

A D V A N C E D K I N E T I C S , I N C .

II.) GENERAL CONSIDERATIONS

A.) THE MODEL

Two aspects of the modeling problem exist: the choice of a representative physical system and the degree to which the mathematics of this system must be simplified to obtain tractable equations which yield meaningful solutions.

Thus the problem arises of the choice of a representative physical system which is complicated enough to enable non-trivial results to be extracted while not being too complicated so as to impede the analytical development. Fortunately, such a system is suggested by strong-field magnet configurations.

In the first place, typical strong-field magnets possess, at least approximately, an axis of symmetry, hence the magnetic field may be taken to be axially symmetric.

Secondly, for pulsed fields the ratio of the period of the field to the period of time spent by the particles in the field may frequently be assumed to be large. Typical field periods are $1 - 10^3$ μsec , whereas the longest particle periods are: 0.05 μsec (1 Kev electron) and 2.0 μsec (1 Kev proton), both particles having a 1m path length in the field. Thus the field may usually be taken to be magnetostatic to a high degree of approximation.

Thirdly, pulsed high field magnets concentrate their fields within certain regions along the symmetry axis, frequently displaying a symmetry about an "equatorial" plane perpendicular to the axis at the magnet center. In fact, it is the spatial inhomogeneity thus produced that creates the injection problem. In such configurations, the field magnitude is zero at $\pm \infty$ along the

A D V A N C E D K I N E T I C S , I N C .

axis and gradually rises to a local maximum at the magnet center. This behavior is adequately represented for the present purposes by a magnetic field of the type whose axial dependence is given by the "bell-shaped" curve.

$$B(0, 0, z) = B_0 / 1 + (z/a)^2 \quad (1)$$

where the z axis is the axis of symmetry and the a denotes the half-width of the field intensity curve at half-maximum. This field has the advantage that many of its properties are amenable to analytic treatment⁴.

Lastly, the ratio of the mean free path of the particles in the beam or bunch to the local gyromagnetic radius will be assumed to be large; space charge effects will be ignored. Roughly speaking, for instantaneous particle currents of a few milliamperes and kinetic energies of at least a few Kev there is no space charge problem. To verify this remark and to estimate these effects more closely, consult Lopukhin⁵. Here the beam will be taken to be an aggregate of single particles.

The simplifications necessary to establish a tractable mathematical model are considerably more restrictive in nature than those introduced above. Since the exact differential equations of motion of a classical structureless point charged particle moving in a magnetostatic field have never been integrated completely⁶, one would expect to introduce some simplification to obtain analytic results. The main assumptions introduced here are two: radiation reaction forces may be neglected, and only the paraxial motion will be considered.

A D V A N C E D K I N E T I C S , I N C .

The neglect of the radiation reaction forces actually involves two separate conditions, since there are both relativistic and nonrelativistic contributions to these forces. By restricting consideration to nonrelativistic motion ($v/c = \beta \ll 1$) the exact differential equations of motion reduce to the following⁶:

$$dv/dt = e/m \ v \times B = (1/d)(d^2v/dt^2) \quad (2)$$

where

$$1/d = e^2/6\pi \epsilon_0 \ mc^3 \quad (3)$$

and where the right-hand side is the well-known nonrelativistic contribution to the radiation force. Further analysis shows that this contribution may be neglected when⁶

$$\omega^2 \ll d/T_p \quad (4)$$

where ω is the gyromagnetic (cyclotron) frequency, T_p is the time which the particle spends in the field. By using the definition of the gyrofrequency

$$\omega = eB/m \quad (5)$$

the inequality (4) may also be written as

$$B^2 \ll (m/e)^2 \ d/T_p \quad (6)$$

This restriction may be shown to be mild for the type of motion considered here, though the restriction is more severe for particles of low mass than for particles of high mass. It should be noted that longer path lengths, such as would be encountered in a mirror device, could make the neglect of the radiation reaction force become a serious error.

A D V A N C E D K I N E T I C S , I N C .

The second simplifying assumption leads to the analysis of paraxial motion, The restrictions involved in this assumption are three:

- 1) the particle trajectory radius (the deviation of the trajectory from the field axis) must be small compared to a characteristic dimension of the field source, denoted by a

$$r \ll a \quad (7)$$

- 2) the slope of the trajectory must be small:

$$dr/dz \ll 1 \quad (8)$$

and

- 3) the ratio of the gyromagnetic radius to a characteristic field length must be large compared to the vector potential

$$mv/eaB \gg A_e \quad (9)$$

The effect of these restrictions on the particle motion is best discussed after the trajectories have been obtained.

It is clear that the particles may penetrate to high field regions in an axially symmetric magnetostatic field when injected on the axis with zero slope because the Lorentz force is zero there and the particles pass through the field undeviated. Such a path is uninteresting because the field does not influence the particle motion at all. A particle injected off-axis with zero slope or on-axis with a small slope will, however, be acted upon by the magnetic field and will pass through the field provided certain conditions are fulfilled. It is the approximate delineation of these conditions and of the high field behavior of the particles that is the object of the present study, and it is here that the paraxial approximation proves useful.

A D V A N C E D K I N E T I C S , I N C .

The physical-mathematical model is now complete. The results presented below are based on the study of the nonrelativistic paraxial motion, neglecting radiation reaction, of a single charged particle moving in an axially symmetric, magnetostatic field whose axial variation is bell-shaped.

B) UNITS

It is necessary in order to obtain the greatest clarity of exposition to adopt a simple, yet physical, system of units for the variables involved in the theory. The system studied requires for its complete characterization the specification of eleven parameters which may be taken as follows: the charge e and the mass m of the particles, the injection point values of the variables $(q_{i0}, \dot{q}_{i0}, t_0 (i = 1, 2, 3))$, a characteristic field value and a field extent parameter. Although a more complex field may involve any number of spatial parameters, the bell-shaped field involves only one, which is taken to be a , the half-width at half-maximum of the axial field curve. The logical choice for the characteristic field value is then B_0 , the maximum axial field value.

The dynamical formulation may be completely freed of its explicit dependence on the system parameters by an appropriate choice of units. The choice made here is as follows:

$$\begin{aligned} \text{Length:} & \quad a \\ \text{Magnetic Field:} & \quad B_0 \\ \text{Time:} & \quad b = m/eB_0 \end{aligned} \tag{10}$$

A D V A N C E D K I N E T I C S , I N C .

Note that time is now measured in units of the reciprocal gyromagnetic frequency with respect to the field center.

The natural coordinate system to employ for the investigation of a general axially symmetric field is the standard circular cylindrical system (r, θ, z) , or (ρ, θ, ζ) in terms of the dimensionless coordinates defined by the equations*:

$$\begin{aligned}\rho &\equiv r/a \\ \zeta &\equiv z/a\end{aligned}\tag{11}$$

* Dimensionless quantities will consistently be denoted by Greek Symbols.

Thus the dimensionless time and velocity take the form

$$\begin{aligned}\tau &\equiv t/b \\ \vec{v} &\equiv m \vec{v} / eaB_0\end{aligned}\tag{12}$$

while the magnetic field and vector potential become:

$$\begin{aligned}\vec{\Gamma} &\equiv \vec{B} / B_0 \\ \vec{a} &\equiv \vec{A} / aB_0\end{aligned}\tag{13}$$

A very convenient aspect of the above definitions is that the magnitude of the dimensionless velocity, v , is in fact the dimensionless gyromagnetic radius of the particle at the field center, assuming the velocity vector to be entirely in the equatorial plane.

$$v = mv/eaB_0\tag{14}$$

This quantity is one of the two most important trajectory parameters. It is here that the advantage of strong magnetic fields is apparent, for high velocities may be used and v may be still kept relatively small, allowing the influence of the magnetic field to be felt.

A D V A N C E D K I N E T I C S , I N C .

III.) FORMULATION OF THEORY

A.) FORBIDDEN ZONES

The concept of the forbidden zones was introduced by C. Störmer (7) in connection with the problem of the motion of a charged particle in the geomagnetic field. The following generalized treatment presents a formulation tailored to the problem to be investigated.

The Lagrangian point of view will be adopted here as the basis for the dynamical formulation. The nonrelativistic Lagrangian for a single charged particle moving in a magnetostatic field is known to be:

$$L = 1/2 m v^2 + e v \cdot A \quad (15)$$

On introducing the variables defined above and denoting the dimensionless Lagrangian by:

$$\Lambda \equiv m L / (e a B_0)^2 \quad (16)$$

the expression (15) for the Lagrangian becomes:

$$\Lambda = 1/2 u^2 + u \cdot a \quad (17)$$

Since it can be shown that the magnetic vector potential of an axially symmetric magnetostatic field may be specified completely by a vector with only an azimuthal component, the basic Lagrangian takes the form:

$$\Lambda = 1/2 (\dot{\rho}^2 + \rho^2 \dot{\theta}^2 + \dot{z}^2) + \rho \dot{\theta} \alpha(\rho, z) \quad (18)$$

It is evident that θ is a cyclic variable, hence the corresponding momentum is conserved:

$$\rho^2 \dot{\theta} + \rho \alpha(\rho, z) = \gamma = \text{const.} \quad (19)$$

A D V A N C E D K I N E T I C S , I N C .

Furthermore, the kinetic energy is conserved because the field is magneto-static:

$$\dot{\rho}^2 + \rho^2 \dot{\theta}^2 + \dot{\zeta}^2 = v^2 = \text{const.} \quad (20)$$

(Note that the kinetic energy is defined here to be one-half of the left-hand side of equation (20)). Eliminating θ between the preceding two equations, the following expression is obtained:

$$\dot{\rho}^2 + \dot{\zeta}^2 + \left(\frac{\gamma}{\rho} - \alpha \right)^2 = v^2 \quad (21)$$

Clearly

$$\left(\frac{\gamma}{\rho} - \alpha \right)^2 \leq v^2 \quad (22)$$

Note that when the equality sign holds in (22) the ρ and ζ velocities are zero, the velocity is entirely azimuthal, and a two-parameter family of curves is defined in the meridional plane:

$$\gamma/\rho - \alpha(\rho, \zeta) = \pm v \quad (23)$$

These curves are the boundaries of the forbidden zones; they delineate those regions of the (ρ, ζ) plane which are inaccessible to particles characterized by the parameters (v, γ) .

B) PARAXIAL FORBIDDEN ZONES

Although equation (23) defines the forbidden zones, it does so implicitly for any field once the axial field variation is known. In spite of the fact that the vector potential for the bell-shaped field is known in closed form (see Glaser⁴) and that the exact zones may be obtained analytically⁸, it is convenient to limit the present discussion to a consideration of the paraxial zones.

A D V A N C E D K I N E T I C S , I N C .

It is well known that the vector potential of an axially symmetric magnetostatic field may be represented as a series expansion about the symmetry axis⁴:

$$\alpha(\rho, r) = \frac{\rho}{2} \sum_{n=0}^{\infty} \frac{(-1)^n}{n!(n+1)!} \frac{d^{2n} \Gamma(\zeta)}{d\zeta^{2n}} \left(\frac{\rho}{2}\right)^{2n} \quad (24)$$

$$= \frac{\rho}{2} \left[\Gamma(\zeta) - \frac{\rho^2}{8} \left(\frac{d^2 \Gamma(\zeta)}{d\zeta^2} \right) + \dots \right] \quad (25)$$

where $\Gamma(\zeta)$ denotes the axial variation of the dimensionless field magnitude:

$$\Gamma(\zeta) \equiv 1/B_0 \sqrt{\vec{B} \cdot \vec{B}} \quad (26)$$

If the axial field variation is reasonably smooth and

$$\rho^2 \ll 1 \quad (27)$$

the first term in the expansion will give a good approximation to the vector potential. This first term is the paraxial vector potential, $\alpha_0(\rho, r)$:

$$\alpha_0(\rho, r) = \frac{\rho}{2} \Gamma(\zeta) \quad (28)$$

and the paraxial forbidden zones are derived by substituting expression (28) into equation (23):

$$\gamma/\rho - (\rho/2) \Gamma(\zeta) = \pm u \quad (29)$$

The explicit form of the zones $\rho(\zeta)$ is given now by the solutions of the quadratic equation

$$\frac{\Gamma(\zeta)}{2} \rho^2 \pm u \rho - \gamma = 0 \quad (30)$$

Since γ may be positive or negative and the solution to the quadratic introduces two more sign possibilities besides the two already evident in equation (30), there are eight roots, which may be denoted by ρ_{abc} ,

A D V A N C E D K I N E T I C S , I N C .

where a refers to the sign of the first degree term in equation (30), b refers to the sign of γ and c refers to the sign introduced by the form of the solution to the quadratic. After excluding the unphysical roots (corresponding to ρ negative real or complex), the following four roots are left:

$$\rho_{+++} = \frac{u}{\Gamma(\zeta)} \left[-1 + \sqrt{1 + 2\bar{\gamma} \Gamma(\zeta)/u^2} \right] \quad (31)$$

$$\rho_{-++} = \frac{u}{\Gamma(\zeta)} \left[1 + \sqrt{1 + 2\bar{\gamma} \Gamma(\zeta)/u^2} \right] \quad (32)$$

$$\rho_{--+} = \frac{u}{\Gamma(\zeta)} \left[1 + \sqrt{1 - 2\bar{\gamma} \Gamma(\zeta)/u^2} \right] \quad (33)$$

$$\rho_{---} = \frac{u}{\Gamma(\zeta)} \left[1 - \sqrt{1 - 2\bar{\gamma} \Gamma(\zeta)/u^2} \right] \quad (34)$$

where $\bar{\gamma}$ indicates the magnitude of γ . Note that when $\gamma = 0$, ρ_{+++} and ρ_{---} both vanish, whereas ρ_{-++} and ρ_{--+} coalesce to give a single zone curve

$$\rho_0 = 2u / \Gamma(\zeta) \quad (35)$$

and the zones are seen to be contour lines of the vector potential. Certain general features of these zones will now be pointed out briefly.

It is clear from equations (31) and (32) that solutions are possible for all values of ζ (for all values of $\Gamma(\zeta)$) when γ is positive, whereas solutions for negative γ are possible only for those values of r for which

$$\Gamma(\zeta) \leq u^2 / 2\bar{\gamma} \quad (36)$$

or for

$$\zeta^2 \geq 2\bar{\gamma}/u^2 - 1 \quad (37)$$

A D V A N C E D K I N E T I C S , I N C .

If

$$2\bar{\gamma}/v^2 \leq 1 \quad (38)$$

then both branches of the negative γ forbidden zone exist for all values of ζ because the inequality (37) is trivially true. However, if

$$2\bar{\gamma}/v^2 > 1 \quad (39)$$

then there exists a lower limit on ζ , given by

$$\zeta = \pm \sqrt{2\bar{\gamma}/v^2 - 1} \quad (40)$$

for which the forbidden zone exists. At this point the equality sign holds in (36) and

$$\rho_{--+} = \rho_{---} \quad (41)$$

Thus it becomes clear that ρ_{--+} and ρ_{---} are simply different branches of the same curve, ρ_{--+} always being larger than ρ_{---} , except at their point of intersection. No such problem arise for positive γ . ρ_{+++} and ρ_{++-} exist for all values of ζ , they never intersect, and

$$\rho_{--+} > \rho_{+++} \quad (42)$$

In fact,

$$\rho_{--+} - \rho_{+++} = 2v/\Gamma(\zeta) \quad (43)$$

Now as $\zeta \rightarrow \infty$,

$$2\bar{\gamma}\Gamma(\zeta)/v^2 \rightarrow 0 \quad (44)$$

and the square roots in equations (31) - (34) may be expanded by the binomial theorem to give

$$\rho_{+++} \sim \bar{\gamma}/v \quad (45)$$

A D V A N C E D K I N E T I C S , I N C .

$$\rho_{-++} \approx 2^U / \Gamma(\zeta) + \bar{v}/U \quad (46)$$

$$\rho_{--+} \approx 2^U / \Gamma(\zeta) - \bar{v}/U \quad (47)$$

$$\rho_{---} \approx \bar{v}/U \quad (48)$$

These relations show that for large ζ the roots ρ_{+++} and ρ_{---} are governed largely by the angular momentum, whereas ρ_{-++} and ρ_{--+} are governed largely by the magnetic field. Since the paraxial approximation has limits for some value of ρ for every value of ζ within which it can reasonably be applied, and since the roots values given by equations (45) and (46) blow up as $\zeta \rightarrow \infty$, the corresponding zones should be employed with discretion (see discussion below on the inaccuracies introduced by employing the paraxial approximation).

Note that the zones given by equations (45) and (48) (and the corresponding more accurate expressions (31) and (33)) appear only as a result of the particle having non-zero angular momentum about the symmetry axis. These zones are the centrifugal barrier zones which arise from the contribution of the centrifugal potential to the meridional plane potential and prohibit the particle from reaching the axis. The other zones, given by equations (32) and (34), arise mainly from the vector potential contribution to the meridional plane potential which acts to prevent the particle from approaching more closely to the field source than its kinetic energy will allow. (The closer the field source is approached, the higher does the magnetic field become; this action forces the particle away from the high field regions and creates the major part of the injection problem).

A D V A N C E D K I N E T I C S , I N C .

More details on the forbidden zones will be given in the section below which deal with the injection conditions. Attention will now be turned to the background for the derivation of the paraxial trajectories.

C.) THE MERIDIONAL PLANE POTENTIAL

It is well known that, under the approximations enunciated above, the motion of a charged particle in an axially symmetric magnetostatic field may be considered to take place in the meridional plane which is defined by the axis of symmetry and the instantaneous particle position. As the particle traverses the field the meridional plane rotates with the particle angular velocity. The motion in this plane may be shown to be conservative and to take place under the influence of a meridional plane potential, π , which is here defined as

$$\pi (\rho, r) = 1/2 \left[\gamma/\rho - \alpha (\rho, r) \right]^2 \quad (49)$$

(see Glaser⁴). This decoupling of the meridional and azimuthal motion is made possible by the existence of the second integral of the motion, the angular momentum integral given in equation (19) above. In fact, considering the motion as taking place under the potential π is just a question of interpreting equation (21) above in the proper manner. A good deal of insight into the types of particle motion may be gained by a study of the meridional plane energy relations.

As far as the energy representation is concerned, the particle motion is determined by the parameters (ν, γ) and their associated surfaces in the

A D V A N C E D K I N E T I C S , I N C .

(ρ , ζ , ϵ) space (the energy, ϵ , is visualized as being plotted vertically over the meridional plane). The surface associated with the particle velocity constant, u , is a plane parallel to the meridional plane at $\epsilon = u^2/2$, while the surface associated with the particle angular momentum constant, γ , is the meridional plane potential energy surface $\epsilon = \pi (\rho , \zeta)$. The magnitude of the meridional plane kinetic energy is determined uniquely for each point (ρ , ζ) by the relation

$$1/2 (\dot{\rho}^2 + \dot{\zeta}^2) = 1/2 \left[u^2 - \left(\frac{\gamma}{\rho} - \alpha (\rho , \zeta) \right)^2 \right] = \frac{u^2}{2} - \pi (\rho , \zeta) \quad (50)$$

hence, it is simply equal to the vertical distance between the two surfaces.

Since the forbidden zone boundaries are defined to be the aggregate of those points for which the meridional plane kinetic energy is zero, they are now seen from a geometrical point of view as the curves which constitute the intersection of the u plane with the π surface.

There are two mechanisms represented in the form of π . One is that associated with the magnetic field which gives rise to the presence of the vector potential in π . The other is that associated with the conservation of angular momentum which gives rise to the centrifugal potential contribution to π . As a particle tries to approach either the field source or the symmetry axis, it encounters strong forces which turn it aside, as shown by the increasing slope of the potential. The distance of closest approach to either region depends mainly on the value of the velocity constant, u , for a given field and γ value. If the other injection parameters are kept constant and u is allowed to vary, then the distance of closest approach will be smaller, the larger is the value of u .

A D V A N C E D K I N E T I C S , I N C .

The trichotomy in the forbidden zone types is now shown to be a reflection of the trichotomy in the meridional plane potential types. Three qualitatively different potentials exist corresponding to whether γ is positive, negative or zero. These cases will now be discussed, using the paraxial approximation.

The equatorial plane traces of these potentials are plotted in Fig. 1 for a representative value of γ . $\gamma = 0$, in this case

$$\pi_0^0(\rho, \zeta) = \rho^2/8(1 + \zeta^2)^2 \quad (51)$$

where π_0 denotes the paraxial approximation to π and the superscript indicates the range of values of γ . The potential exhibits a simple variation; it increases as the square of ρ for constant ζ , and decreases away from the equatorial plane as $\Gamma^2(\zeta)$ for constant ρ . $\gamma > 0$ For this case

$$\pi_0^+(\rho, \zeta) = 1/2 \left[\gamma/\rho - \rho/2(1 + \zeta^2) \right]^2 \quad (52)$$

This potential has a zero on the line of force given by

$$\rho \alpha(\rho, \zeta) = \gamma = \rho^2/2(1 + \zeta^2) \quad (53)$$

Since this line corresponds to the allowed zone for $v = 0$, it is seen that for positive γ a line of force is a possible trajectory in the limit of infinitely small velocity. The centrifugal potential contributes strongly as $\rho \rightarrow 0$, and the vector potential contributes strongly as $\rho \rightarrow \infty$. $\gamma < 0$, here

$$\pi_0^-(\rho, \zeta) = 1/2 \left[\bar{\gamma}/\rho + \rho/2(1 + \zeta^2) \right]^2 \quad (54)$$

This potential form has no zeros, but possesses a local minimum on the line of force

$$\rho \alpha(\rho, \zeta) = \bar{\gamma} = \rho^2/2(1 + \zeta^2) \quad (55)$$

A D V A N C E D K I N E T I C S , I N C .

because the derivative with respect to ρ is zero there. Again the contributions from the centrifugal and vector potentials show up as in the positive γ case.

The difference between the positive and negative potentials is

$$\pi_{\circ}^{-} - \pi_{\circ}^{+} = \gamma / (1 + \zeta^2) \quad (56)$$

hence the π_{\circ}^{-} surface is just the π_{\circ}^{+} surface shifted vertically by an amount which varies from γ in the equatorial plane to zero at $\zeta = \infty$ (see Fig. 2, where this difference has been plotted along the line of force given by equation (55) for the same value of γ used for the plots of Fig. 1). This result is useful in the sequel.

The forbidden zone behavior is now easier to understand. Consider the cases of Fig. 1. An allowed zone reaches the equatorial plane in all three cases for values of $u^2/2 \geq 0.0198 = \gamma$, while for $u^2/2 < 0.0198 = \gamma$ only the zero and positive γ zones penetrate to the equatorial plane; this is in accord with equation (38).

D.) THE PARAXIAL TRAJECTORY EQUATION

As a result of the decoupling of the meridional and azimuthal motion, it is possible to find directly a differential equation which the meridional plane trajectory satisfies and which includes only (ρ, ζ) as variables. The Jacobi form of the Principle of Least Action (see Goldstein⁹) here takes the form

$$\delta \int_{\zeta_2}^{\zeta_1} (\mu)^{1/2} \left[\left(\frac{d\rho}{d\zeta} \right)^2 + 1 \right]^{1/2} d\zeta = 0 \quad (57)$$

A D V A N C E D K I N E T I C S , I N C .

where the following definition has been introduced

$$\mu \equiv v^2 - 2\pi(\rho, \zeta) \quad (58)$$

The Euler equation for the variational principle (57) yields the following differential equation for the meridional plane trajectory:

$$\rho'' = (1 + \rho'^2) / 2\mu \left[\frac{\partial \mu}{\partial \rho} - \rho' \left(\frac{\partial \mu}{\partial \rho} \right) \right] \quad (59)$$

Where the prime denotes differentiation with respect to ζ . Since this equation is too complicated to solve in its full generality, the reason for the use of the paraxial approximation in studying the trajectories becomes evident.

The paraxial trajectory equation is obtained from equation (59) by introducing the following assumptions:

- (I) $\gamma = 0$
- (II) $\rho'^2 \ll 1$
- (III) $\rho''^2 \ll 1$
- (IV) $v^2 \gg \pi^2(\rho, \zeta)$

Thus the paraxial trajectory equation for the bell-shaped field becomes

$$\rho''^2 = \rho / 4v^2 (1 + \zeta^2)^2 \quad (60)$$

The solution to this equation was obtained by Glaser¹⁰ in the form

$$\rho = C \sqrt{1 + \zeta^2} \sin \left[\sqrt{1 + 1/4v^2} \cot^{-1} \zeta_0 + \varphi \right] \quad (61)$$

where C and φ are functions of the injection parameters. For particles injected on the axis with injection parameters $(\rho_0, \zeta_0, \rho'_0, v)$ this has been shown to take the form¹¹:

$$\rho = 2v\rho'_0 \sqrt{1 + \zeta_0^2 / 1 + 4v^2} \sqrt{1 + \zeta^2} \sin \left[\sqrt{1 + 1/4v^2} \cot^{-1} \zeta - \cot^{-1} \zeta_0 \right] \quad (62)$$

Only this type of trajectory will be considered here.

A D V A N C E D K I N E T I C S , I N C .

A few pertinent features of these trajectories will be quoted here before proceeding to a consideration of the injection problem (see MacLeod¹¹).

The trajectories are contained within the envelope curve

$$\rho_e = 2u\rho'_0 \sqrt{1 + \zeta_0^2/(1 + 4u^2)} \sqrt{1 + r^2} \quad (63)$$

The trajectory touches the axis N times at the point

$$\zeta_n = \cot \left[\frac{n\pi 2u}{\sqrt{1 + 4u^2}} + \cot^{-1} \zeta_0 \right] \quad (64)$$

n is given by

$$\text{INT} \left[\left(1 + 1/4u^2 \right)^{1/2} \left(1 - (\cot^{-1} \zeta_0 / \pi) \right) \right] \quad (65)$$

where INT (x) signifies the largest integer less than x. The trajectory slope may be shown to have local maxima at the points ζ_n , where the slope is

$$\rho'_n = (-1)^{n+1} \rho'_0 \sqrt{(1 + r_0^2)/(1 + \zeta_n^2)} \quad (66)$$

E.) DEFINITION OF INJECTION PROBLEM

It is now possible to define the injection problem more closely. Since for the given type of field in region in and around the equatorial plane becomes the high field region, as the term is understood here, the injection problem may be stated as follows:

To determine those values of the injection parameters $(t_0; \rho_0; \theta_0; r_0; \dot{\rho}_0; \dot{\theta}_0; \dot{\zeta}_0)$ which will allow the particle to attain the equatorial plane.

It is clear that the initial time may be chosen arbitrarily (the field is magnetostatic and no particle-particle phase effects are considered here), thus t_0 may be taken to be zero.

A D V A N C E D K I N E T I C S , I N C .

Furthermore, the field is axially symmetric, hence the value of θ_0 has no effect on the trajectory behavior in the meridional plane and may be set equal to zero with no loss of generality.

In addition to the foregoing simplifications, it will prove convenient to introduce the trio (ν, γ, ψ) instead of $(\dot{\rho}_0, \dot{\theta}_0, \zeta_0)$, where

$$\psi = \tan^{-1} (d\rho/dr_0) = \tan^{-1} (\dot{\rho}_0/\zeta_0) \quad (67)$$

Thus the aim is to find acceptable values of the set

$$(\rho_0, \zeta_0, \nu, \gamma, \psi) \quad (68)$$

A D V A N C E D K I N E T I C S , I N C .

IV.) RESULTS

It is convenient to distinguish two cases: zero and non-zero γ . Qualitative results on the specification of the injection parameters will be given for both cases through a discussion of the relevant forbidden zones, and quantitative results will be given in addition for the zero γ case by utilizing the paraxial trajectories.

Case 1: $\gamma = 0$

These forbidden zones depend only on the parameter ν . Several of the paraxial zones are depicted in Fig. 3. The allowed region for a particle of parameter ν extends from the axis to the appropriate ν curve. The axis is an allowed region for all values of ν for particles injected with $\rho_0 = 0, \psi = 0, \pi$. However, as soon as ψ becomes non-zero the value of ν must be reckoned with.

For small ν values, the chances of a remotely injected particle ($\zeta_0 \gg 2$) penetrating to the equatorial plane are poor unless ψ is quite small, although there is a trajectory compression mechanism at work which increases the chances over the purely geometrical values. As ν increases the acceptance angle (defined to be the maximum value of ψ which allows equatorial plane attainment) at any given ζ_0 increases. It is not possible, however, to increase ν indefinitely and keep increasing the acceptance angle. According to the paraxial zones the equatorial plane zone radius increases indefinitely as ν is increased;

A D V A N C E D K I N E T I C S , I N C .

this is an error due to the approximation used. Although the paraxial zones do not show it, the field source is located at $\rho = 1.0$ in the equatorial plane, hence the equatorial zone radius should approach 1.0 asymptotically as $u \rightarrow \infty$; only for infinite velocity can the particle reach the field source. Thus the error in the zone boundaries introduced by using the paraxial approximation becomes more and more serious as u increases. A consideration of the second term in the vector potential expansion, equation (25), shows that this term contributes 10% to the vector potential at $\rho \approx 0.63$ (in the equatorial plane). The tolerance of the error in the specification of the zone boundary position varies with the application, but a 10% error will be taken here to be the maximum allowable value. In effect, this limits the range of u which may be used with reasonable confidence because any zone which has an equatorial radius $\rho > 0.63$ has at least a 10% error associated with it. Since the equatorial radius is given by

$$\rho_{eq} = 2u \quad (69)$$

u is limited by the relation

$$u \leq \rho_{eq}/2 \approx 0.30 \quad (10\% \text{ error}) \quad (70)$$

It should be noted, though, that this limitation applies strictly only to those particles which approach the zone boundary in or near the equatorial plane. The choice of the remaining injection parameters (ρ_0, r_0, ψ) can greatly change the limit (70). The extreme example of this is axial injection with $\psi = 0$ or π ; any value of u is acceptable.

A D V A N C E D K I N E T I C S , I N C .

The use of the paraxial trajectories is limited in like manner by the assumptions (I) - (IV) above. Assumptions (III) and (IV) are the most restrictive of the group. According to (IV) the trajectories must not approach the forbidden zones closely. At the very least this means that the trajectory envelope must not intersect the zone boundary. This gives rise to a condition on the injection parameters. Since the envelope is similar to the zone boundary but of smaller curvature everywhere (compare equations (63) and (35)), if the equatorial envelope radius is smaller than the equatorial zone radius the curves will not cross anywhere. Condition (IV) thus becomes in effect

$$\rho_e \ll \rho_o \quad (\text{in the equatorial plane}) \quad (71)$$

or

$$\rho_o' \sqrt{1 + \zeta_o^2 / 1 + 4u^2} \ll 1 \quad (72)$$

which is satisfied by small ρ_o' , small ζ_o or large u . It is interesting that this latter form of condition (IV) turns out to be similar to condition (III).

Since the maximum value of ρ_o is at the n th axis touchpoint, according to equation (66), condition (III) may be formulated as follows:

$$\rho_o' \sqrt{1 + \zeta_o^2 / 1 + \zeta_n^2} \ll 1 \quad (73)$$

which is satisfied by small ρ_o' , small ζ_o or large ζ_n . The worst case corresponds to the particle having one of its axis touchpoints near the field center; then

$$\zeta_n \approx 0 \quad (74)$$

A D V A N C E D K I N E T I C S , I N C .

and

$$\rho'_0 \sqrt{1 + \zeta_0^2} \ll 1 \quad (75)$$

hence condition (III) is generally more stringent than condition (IV), although for small values of u the difference becomes slight.

Although it may seem that condition (II) is the most stringent of all, this is not the case. The purpose of imposing (II) was solely to ensure rapid convergence of the vector potential series; the series may converge rapidly without (II). Such is the case for certain regions of the meridional plane, in fact for the region within which the contribution from the second term is less than a specified small fraction of the leading term, say 0.10. The boundary of this region may be obtained by equating the second term to 0.10 times the leading term and thereby reduces to the equation

$$\rho = 0.632 \frac{H \zeta^2}{\sqrt{|1 - 3 \zeta^2|}} \quad (76)$$

for $\zeta \gg 1$ this becomes

$$\rho = 0.365 \zeta \quad (77)$$

a considerable weakening of condition (II), and the condition that ρ_e be less than this becomes

$$u \rho'_0 \sqrt{1 + \zeta_0^2 / 1 + 4u^2} \lesssim 0.365 \quad (78)$$

A D V A N C E D K I N E T I C S , I N C .

If v is small, this is easily satisfied; if v is large, (78) takes the form

$$\rho_o' \left(1 + \zeta_o^2 \right)^{1/2} \approx 0.730 \quad (79)$$

which is less restrictive than equation (75).

Thus the conditions (II) - (IV) will all be satisfied if equation (75) is valid; this is the basic restriction, and it is serious, though not of unexpected character. For remote injection (75) becomes

$$\rho_o' \ll 1/\zeta_o \quad (80)$$

i.e.,

$$\tan \psi \ll 1/\zeta_o \quad (81)$$

or roughly,

$$\psi \ll 1/\zeta_o \quad (82)$$

The injection angle must be considerably less than the angle subtended by the inner edge of the field source ($\rho = 1.0$, $\zeta = 0$); this was to be expected.

Thus the injection parameter ranges for axial injection are as follows (with the above qualifications):

$$v \gtrsim 0.30 \quad (83)$$

$$\tan \psi \ll 1/\zeta_o \quad (84)$$

and ζ_o is arbitrary, but its choice is influenced by condition (84).

A D V A N C E D K I N E T I C S , I N C .

Case II: $\gamma \neq 0$

The basic question to be answered here is whether there seems to be any advantage to non-zero γ injection which would suggest that it be used in spite of the less detailed knowledge available about trajectory properties. The answer to this question seems to be affirmative.

First of all there is a qualitative difference between positive and negative γ injection (see Figs. 4 and 5 for representative zones). The allowed zones for positive γ extend between the two branches of the zone boundary curves and include the line of force. The allowed zones for negative γ are to the right of the zone boundary curves and include only part of the line of force (no two-branch zones are plotted for negative γ , although they exist when condition (85) below is fulfilled). No particle of negative γ may reach the equatorial plane regardless of the other injection parameter values unless

$$u^2 > 2\gamma \tag{ 85 }$$

This is emphasized by the plot of π_0 along the line of force which is given in Fig. 2. As a particle moves along the line of force toward the equatorial plane π_0 increases rapidly and eventually forces the particle to retreat unless condition (85) is satisfied. Even when this condition is satisfied, part of the particle kinetic energy is expended in overcoming this equatorial barrier potential. On the other hand, if the other injection parameters have appropriate values, a particle of positive γ is highly preferable to injection with negative γ .

A D V A N C E D K I N E T I C S , I N C .

Secondly, the forbidden zone is approached as the azimuthal velocity is increased when the particle nears the equatorial plane. Therefore, it would seem advantageous to inject with zero angular velocity in order to increase the chances for the particle to penetrate to the equatorial plane.

Thirdly, injection along a line of force would seem to offer the best chance for equatorial penetration because the meridional plane force on the particle is zero on the line of force. Thus the following condition must be satisfied for line of force injection:

$$\rho_0^2 / 2 (1 + \zeta_0^2) = \gamma \quad (86)$$

Lastly, it is desirable to use a relatively small value of ν to allow the magnetic field to influence the particle in the high field region. A balance must be struck between too large a value of ν (too little field influence) and too small a value of ν (too much field influence).

A D V A N C E D K I N E T I C S , I N C .

- 1.) Furth, H. P., and R. W. Waniek, Rev. Sci. Inst. 27, 195 (1956).
- 2.) Furth, H. P., and R. W. Waniek, Rev. Sci. Inst. 28, 949 (1957).
- 3.) MacLeod, M. A. and R. W. Waniek, Bull. Amer. Phys. Soc. II, 3, 58 (1958).
- 4.) Glaser, W., "Grundlagen der Elektronenoptik," Springer, Vienna, 1952.
- 5.) Lopukhin, V. M., Vozbuzhdenie elektromagnitnykh kolebaniy i voin elektronnyimi potokami (The Excitation of Electromagnetic Oscillations and Waves by Electric Currents), GITTL, Moscow, 1953.
- 6.) Plass, G. N., Revs. Mod. Phys. 33, 37 (1961).
- 7.) Störmer, C., "The Polar Aurora," p. 376, Oxford University Press, London, 1955.
- 8.) MacLeod, M. A., Boston College Dept. of Physics, Plasma Project Progress Report, 1958, unpublished.
- 9.) Goldstein, H., Classical Mechanics, Addison-Wesley, Cambridge, Mass., 1952.
- 10.) Glaser, W., Zeit. f. Physik 117, 285 (1941).
- 11.) MacLeod, M. A., Thesis, Brandeis University, Waltham, Mass., 1958.

FIGURE-1
BELL SHAPED FIELD
EQUATORIAL PLANE VARIATION
of
PARAXIAL MERIDIONAL PLANE POTENTIAL

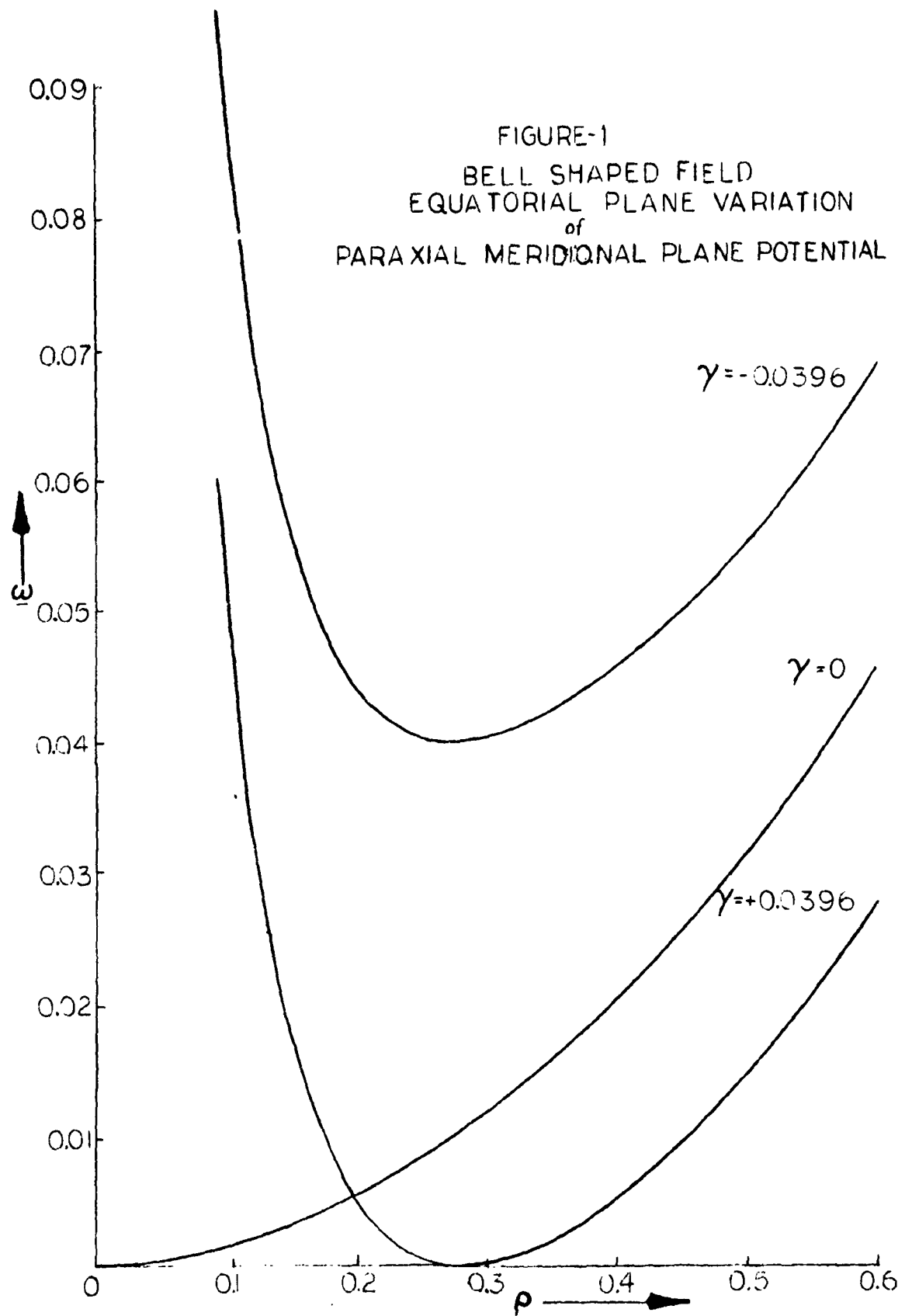
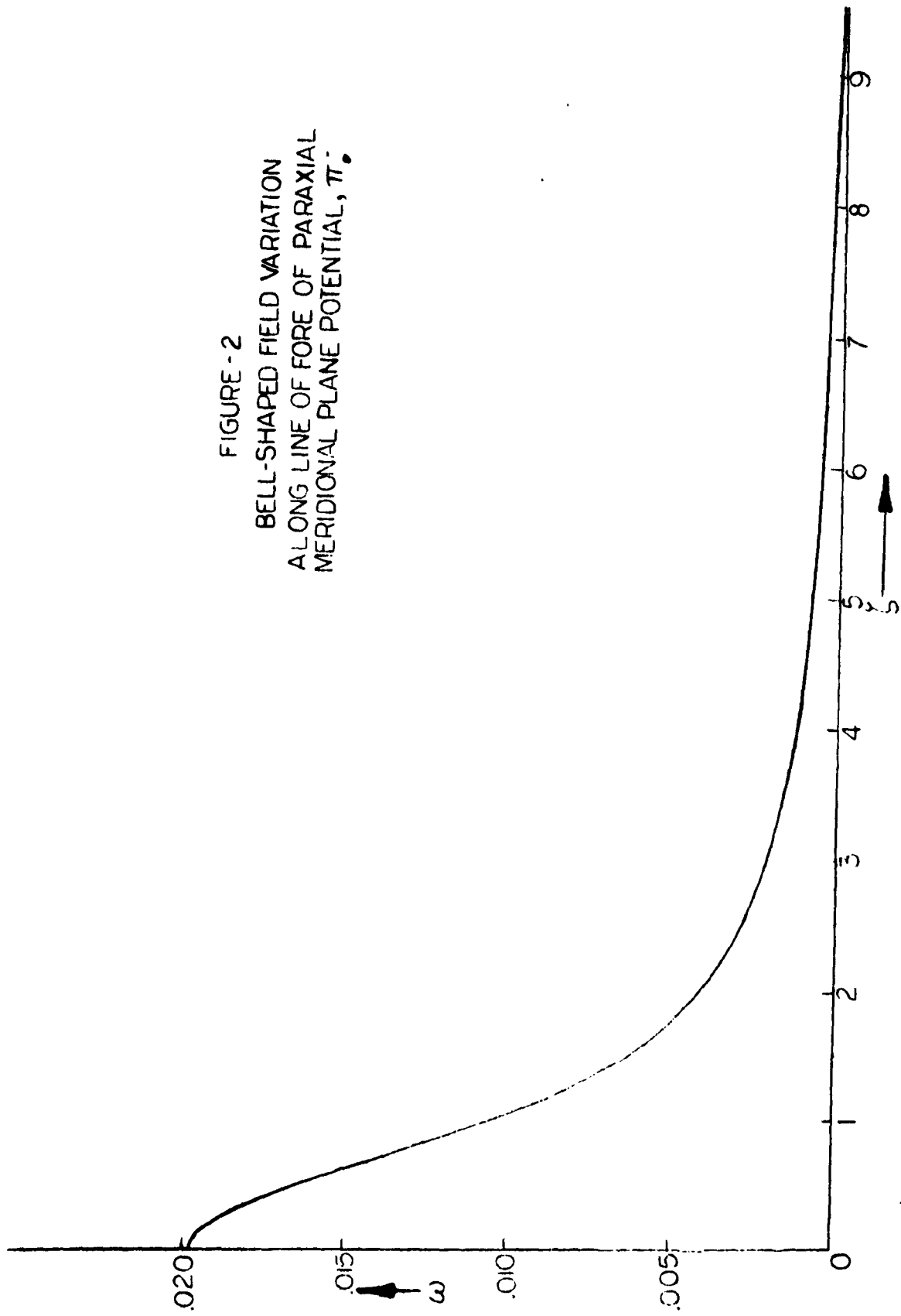


FIGURE - 2
BELL-SHAPED FIELD VARIATION
ALONG LINE OF FOC OF PARAXIAL
MERIDIONAL PLANE POTENTIAL, π .



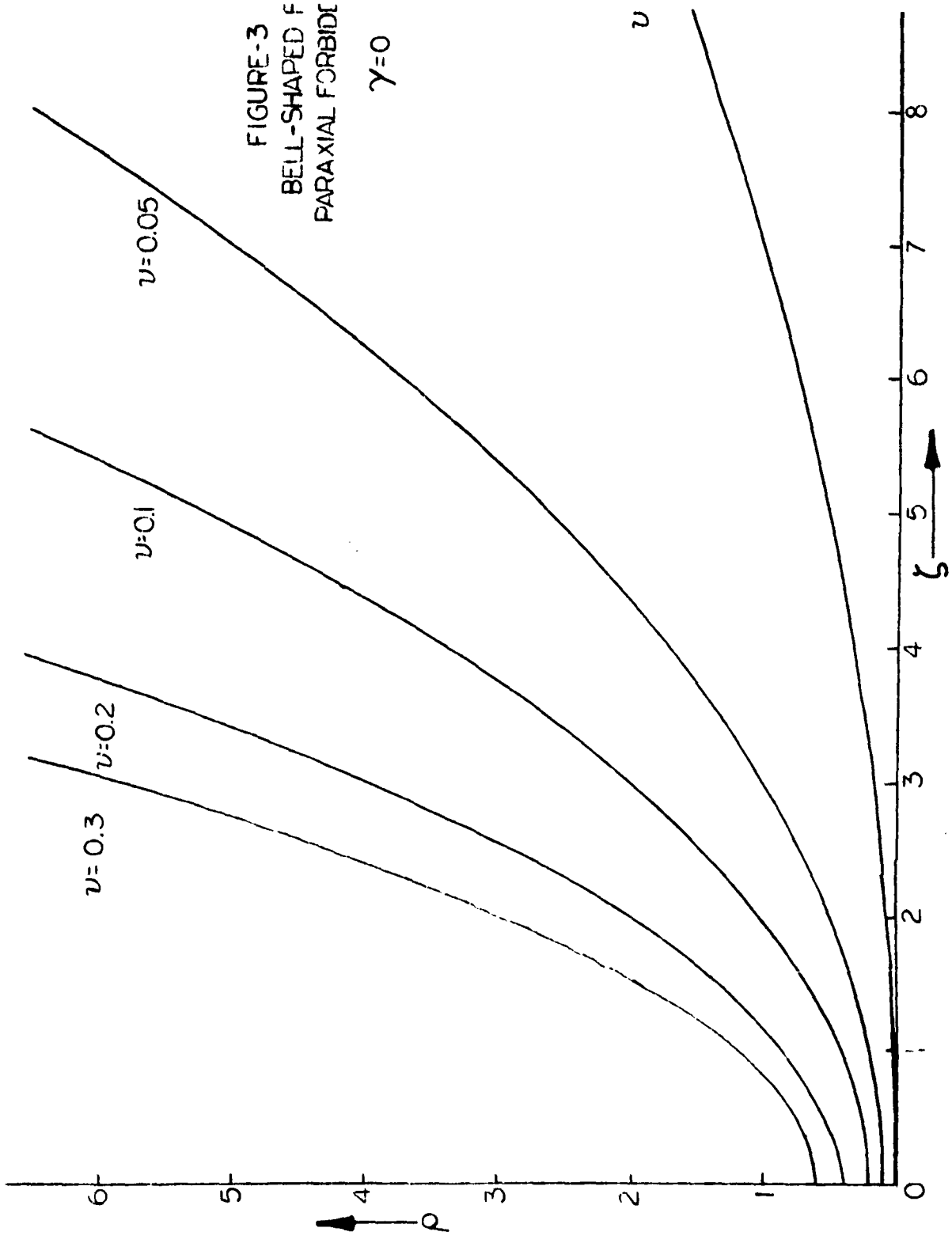


FIGURE-3
 BELL-SHAPED F
 PARAXIAL FORBIDE
 $\gamma=0$

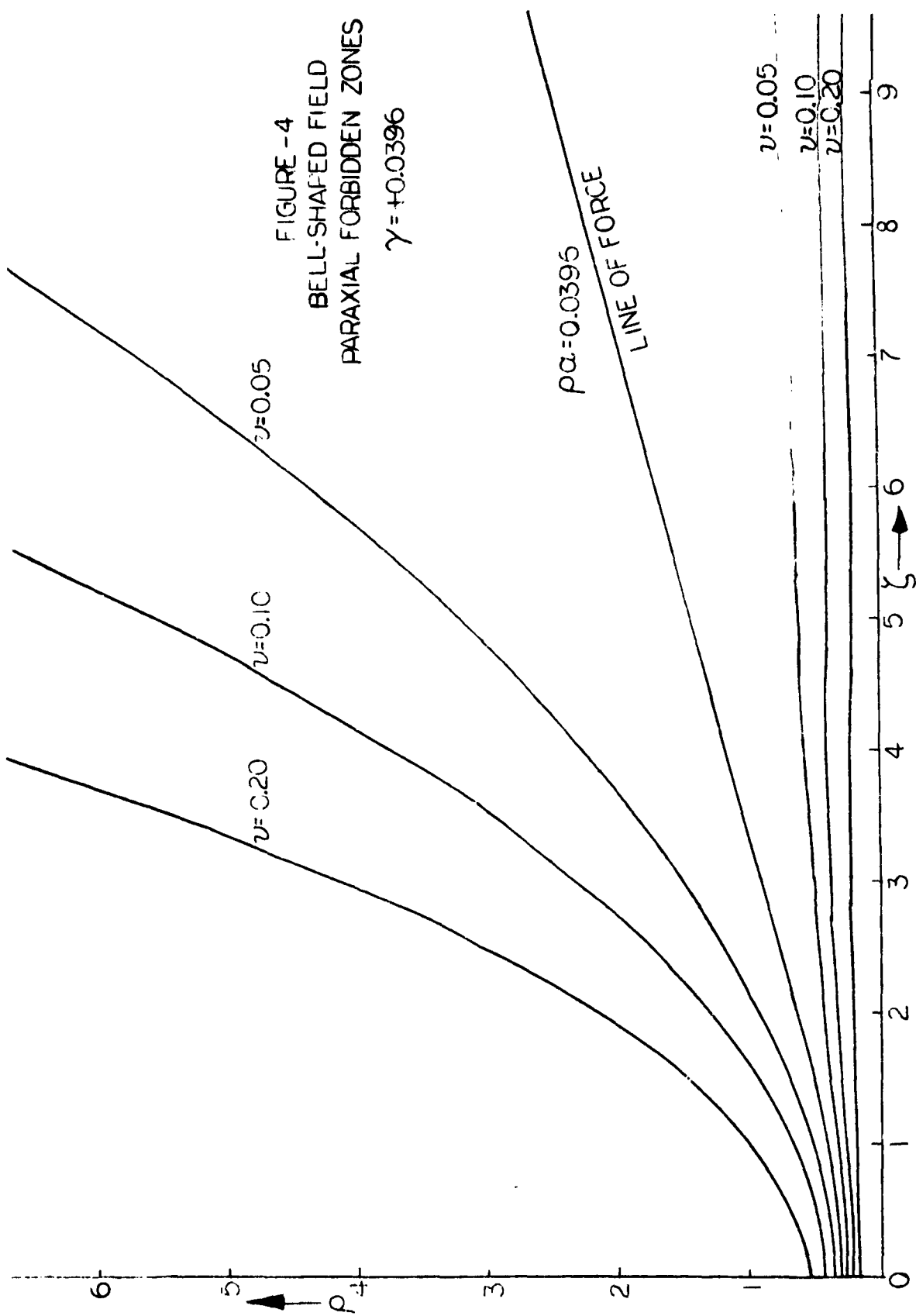


FIGURE -4
 BELL-SHAPED FIELD
 PARAXIAL FORBIDDEN ZONES
 $\gamma = +0.0396$

$\nu = 0.05$
 $\nu = 0.10$
 $\nu = 0.20$

$\rho_\alpha = 0.0395$
 LINE OF FORCE

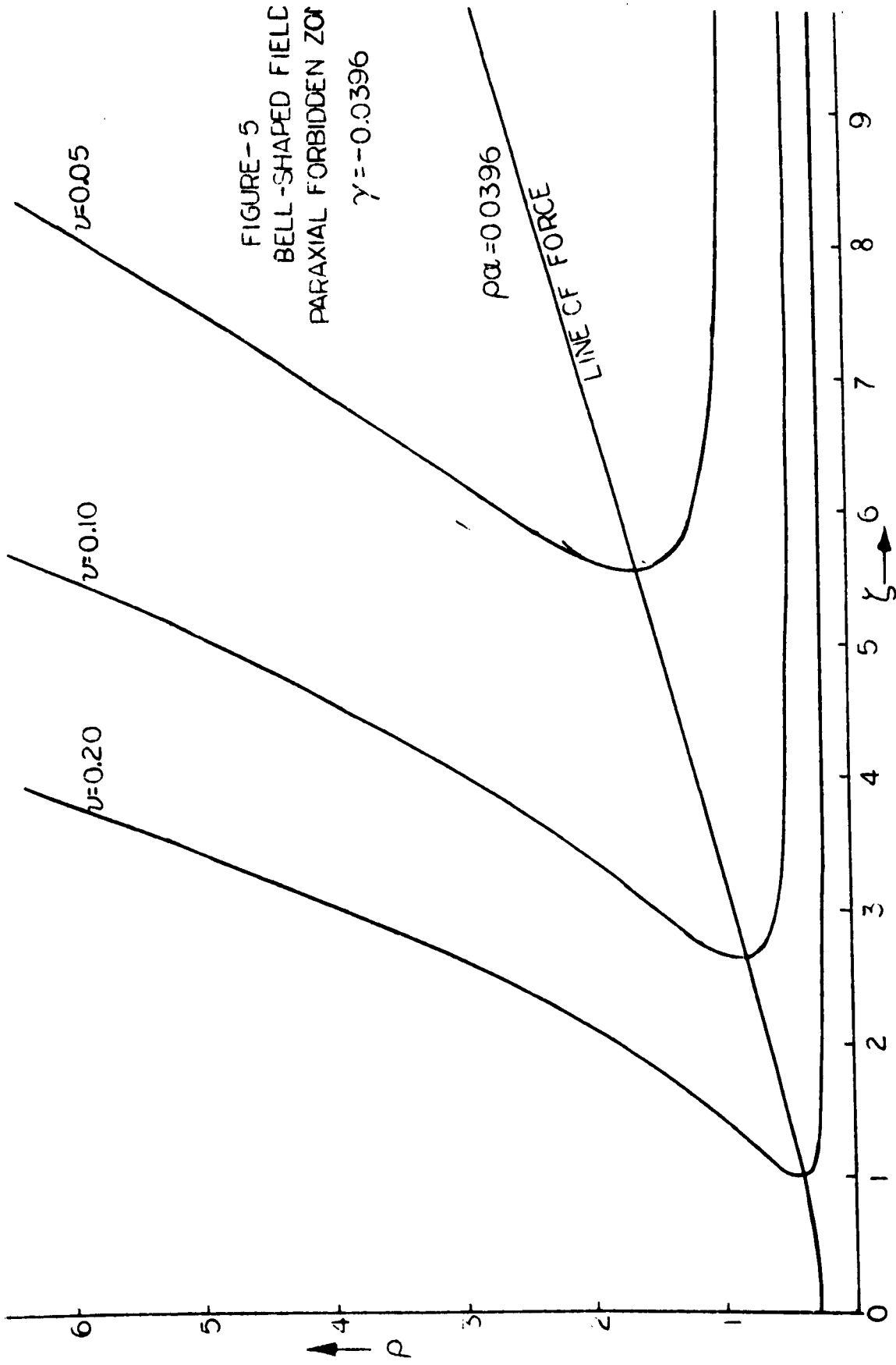


FIGURE-5
 BELL-SHAPED FIELD
 PARAXIAL FORBIDDEN ZONE